Article

SHOALS Object Detection

By Eric Yang and Paul E. LaRocque (Canada)
Optech Incorporated, 300 Interchange Way, Vaughan
Ontario, Canada

Abstract

For the past decade, SHOALS (Scanning Hydrographic Operational Airborne Lidar Survey) has proven to be an efficient and cost-effective means for large-area coastal mapping projects. However, its capabilities in the rapid reconnaissance of small underwater obstructions have been less appreciated, despite a demonstrated history of successful detection and spatial identification. This paper discusses SHOALS' object detection capabilities in light of the recent developments in object detection algorithms, with multiple situation studies to illustrate its overall performance and latest enhancements. Various aspects of object detection using airborne bathymetric lidar are discussed to highlight the challenges and advantages of using SHOALS for rapid reconnaissance of small underwater obstructions.

Résumé

Au cours de la dernière décennie, SHOALS (Scanning Hydrographic Operational Airborne Lidar Survey) s'est révélé être un instrument efficace et rentable en ce qui concerne les projets de cartographie côtière à grande échelle. Toutefois, ses capacités en matière de reconnaissance rapide des petites obstructions sous-marines ont été moins appréciées malgré des antécédents avérés de détection réussie et d'identification spatiale. Cet article traite des capacités de détection d'objet du SHOALS à la lumière des récents développements intervenus dans les algorithmes de détection d'objets, avec de nombreuses études de situations qui illustrent l'ensemble de ses performances et les dernières améliorations. Divers aspects de la détection d'objets à l'aide du lidar bathymétrique aéroporté ont été abordés dans le but de souligner les défis et les avantages de l'utilisation du SHOALS pour la reconnaissance rapide des petites obstructions sous-marines.

Resumen

Durante la última década, SHOALS (Scanning Hydrographic Operational Airborne Lidar Survey) ha demostrado ser un medio eficaz y económico en lo que se refiere a proyectos de cartografía costera a gran escala. Sin embargo, sus capacidades en materia de reconocimiento rápido de pequeñas obstrucciones submarinas han sido menos apreciadas, a pesar de los antecedentes manifiestos de una lograda detección y de una identificación espacial. Este artículo trata sobre las capacidades de detección de objetos del SHOALS a la luz de los recientes desarrollos acaecidos en los algoritmos de detección de objetos, con múltiples estudios de situaciones para ilustrar su funcionamiento general y sus últimas mejoras. Se han abordado varios aspectos de la detección de objetos que utilizan el lidar batimétrico aerotransportado para destacar los retos y las ventajas del uso del SHOALS para un reconocimiento rápido de pequeñas obstrucciones submarinas.

1. Introduction

One of the fundamental requirements of hydrographic surveys is to detect underwater objects or obstructions. IHO-1 surveys require that all features larger than 2-m cubes be identified in water depths up to 40 m, whereas the corresponding requirement for IHO Special Order is to detect 1-m cubes (IHO 2008).

Although SHOALS has been widely accepted as an efficient and cost-effective means for large-area coastal mapping projects, whose depth measurement accuracy meets and exceeds IHO-1 requirements (Lockhart et al. 2005; LaRocque et al. 2004), there has been considerable debate over its capabilities in the rapid reconnaissance of small underwater obstructions and targets, partly because of misunderstanding and ambiguity in communication. It can be argued that poor perception, rather than technological limitations, has been the limiting factor on applications of airborne lidar in hydrographic surveys (West, Lillycrop 1999).

Since the ability to detect underwater objects is crucial for SHOALS to perform as a fully functional hydrographical survey tool, Optech has made further efforts to improve SHOALS' object detection capability. Test results revealed that SHOALS is not only capable of reliably detecting 2-m cubes to meet IHO-1 requirements, but also capable of consistently detecting 1-m cubes under normal clean water conditions and potentially 0.5-m cubes under ideal circumstances.

This paper will examine SHOALS' enhanced object detection capability, and provide both analytical and empirical results. The analytical discussions are based on the sensor configuration and associated parameters of the current SHOALS-3000 system. Case studies are presented to illustrate automatic identification of underwater features using the SHOALS ground control software (GCS).

2. Overview of SHOALS object detection

In bathymetric lidar, many factors contribute to the ability and probability of detecting underwater objects, including water depth, water clarity, object dimensions, object/bottom reflectivity, system configuration, survey planning, and data processing, as well as sophisticated algorithms to automatically identify underwater anomalies.

One of the most obvious factors affecting bathymetric lidar surveys is water clarity, which not only limits the maximum measurable depth, but also considerably affects underwater object detectability. For detecting underwater objects with limited dimensions, lidar point density also plays a significant role. In general, two key factors define object detectability: 1) the probability that the object will be illuminated (wholly or partly) by the laser footprint, which depends on the effective laser footprint size and lidar point density; 2) the ability to identify the object return signal from its surroundings, which depends on the significance of the object return signal and the sensitivity of the object detection algorithm to discern object signatures.

In practice, the criteria for selecting objects from various bottom anomalies and features (with variable dimensions) also play a part in the final result of object identification. This can sometimes cause confusion when comparing detection lists from different methods or from those manually selected by different individuals. We distinguish between object detection, which depends upon the hardware parameters, environmental conditions and algorithms, and object selection, which is more dependent upon subjective items such as the methodology and selection criteria. The focus of this paper is more on object detection.

In 1996, an analytical study was conducted on the performance of bathymetric lidar in underwater obstruction detection, based on parameters and algorithms in use at that time (Guenther *et al.* 1996). Multiple scenarios with different object dimensions, water conditions, and lidar point densities were discussed in that study, which resulted in predictions of target detection probabilities under various scenarios for the SHOALS system. As an example, ***Figure 1*** shows the analytical results of detection probabilities for 4-m^2 circular cylinders in various water clarities, with 1-m and 2-m target heights, using 4 m × 4 m lidar point density. Apparently, objects with 2-m height and 4-m^2 surface area can be detected with almost unit probability in clear water conditions, even with 4 m × 4 m spot spacing, which meets IHO-1 requirements. It is noteworthy that the criteria for positive object identification are based on either distinctive bottom peak separation (Type-1 detection) or a correct reading of least depth from the merged bottom peak (Type-2 detection). Type-1 detection occurs when the return signals from both the object and the water bottom can be discerned separately and measured using the traditional depth extraction algorithms. Type-2 detection occurs when the return signal from the target surface area overshadows that of the water bottom.

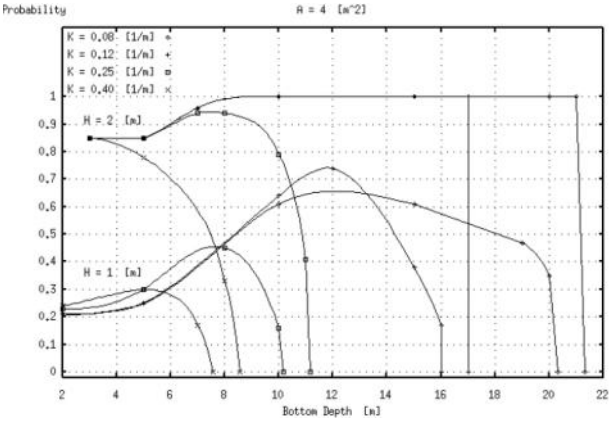

Figure 1: Detection probabilities for 4-m^2 circular cylinders in various water clarities, with 1-m and 2-m target heights, using a 20° nadir angle and 4 m × 4 m lidar point density (Guenther et al 1996).

The practical experience of several SHOALS users supported and frequently exceeded the performance expectation of the analytical predictions and demonstrated that airborne lidar bathymetry is commonly capable of detecting small features and objects to meet IHO-1 requirements (West, Lillycrop 1999) (Guenther 2007) (Lockhart *et al.* 2005).

One of the unique design parameters of SHOALS was to have two depth channels. One was optimized for deep water to 50 meters and one was optimized for shallow water from zero to ~ 17 meters. The deep channel has a large receiver Field of View (FOV) and the shallow depth channel has a smaller FOV of ~ 15 mrad. This enhances object detection capability as discussed later.

Since 1996, SHOALS has undergone substantial upgrades in hardware, software and algorithms (LaRocque *et al.* 2004) (LaRocque *et al.* 2005) (Yang *et al.* 2007), which has also enhanced its performance in underwater object detection. With the addition of higher point densities, up to 2 m × 2 m spot spacing, the geometric searching capability has drastically improved, with virtually 100% bottom illumination by a single coverage. Most important, Optech's latest efforts to improve the object detection algorithm, whose predecessor was merely a by-product of traditional depth extraction algorithms, have revealed that the SHOALS system is much more capable than was initially predicted (Guenther *et al.* 1996) in terms of object resolution and detectability when the sophisticated algorithm is used. The significant enhancement in SHOALS' object detection capability is therefore primarily due to algorithmic advances in identifying abnormal bottom returns, with experience built upon Optech's latest success with the shallow water algorithm (SWA) (Yang *et al.* 2007).

3. Enhanced object detection and categorization

3.1. Enhanced object detection

The SHOALS laser beam strikes the air/water interface with a footprint size of about 2 m and a constant incident angle of about 20° (LaRocque *et al.* 2004).

Although such a configuration originally considered eye-safety, depth penetration, water surface detectability, and minimization of propagation biases, it is also beneficial for underwater object detection in terms of geometric searching, object differentiation and consistency across the scan swath. Because the laser beam further expands in the water column, often significantly, owing to scattering from entrained particulates, it ensures that 100% bottom illumination is achievable even with a lesser lidar point density, such as 3 m × 3 m. Furthermore, with the current configuration of the SHOALS-3000 system, the programmable scanner patterns allow lidar point density to vary from 2 m × 2 m to 5 m × 5 m (LaRocque, Yang 2010) (***Table 1***). This means that SHOALS-3000 is virtually a complete bottom imager from shallow to deep water, capable of illuminating single rocks or objects sitting on top of a relatively flat bottom surface.

If 100% bottom illumination is assured by using suitable point density patterns, object detectability relies on the capability of identifying an object from its return signal, which is usually compounded by the return signal from the water column and bottom. Traditionally, the approach to identifying an object involves resolving distinguishable return signals from both the object and bottom. This works in cases where the object dimensions are greater than what can be resolved by the traditional pulse location algorithms (Guenther *et al.* 1996). Because the laser footprint is usually greater than 2 m in diameter when reaching the bottom, depending on water depth and water properties, objects the size of 2-m cubes (or smaller) are usually covered entirely by laser footprints, introducing distortions to the return signal normally dominated by the bottom return signal. If such distortion is significant enough to produce a separate and resolvable return signal from the object surface, it will be recognized as an object by the traditional method. In cases where an object is significantly larger than the laser footprint, the return signal from the object may be reflected entirely from the top of the object with no sign of distortion.

Table 1: Scan patterns for SHOALS-3000

Nominal Spacing (m)	Altitude (m)	Swath (m)	Lateral Spacing (m)	Forward Spacing (m)	Speed (knots)	Coverage (km^2/hr)
2 x 2	400	160	2	2	126	37
	300	150	2	2	130	36
3 x 3	400	300	3	3	125	70
	300	225	3	3	165	69
4 x 4	400	300	4	4	220	122
	300	225	3.5	4	255	106
5 x 5	400	300	4.5	4.4	275	153

However, such objects will also be identified in the lidar point clouds because of their raised elevations. In general, objects larger than the laser footprint will always be captured, whereas objects comparable to the size of the laser footprint will usually be recognized by the traditional method of object identification.

The traditional method of object detection is limited by its ability to identify smaller objects that are insufficient to produce separate object and bottom returns. ***Figure 2*** shows two waveforms from two underwater objects sitting side by side at a depth of about 9 m. These two targets were man-made objects with known dimensions.

In ***Figure 2*** the waveform on the left is from a 1-m cube, whereas the waveform on the right is from a 2-m cube. The 2-m cube produced clear separation between the bottom return (marked with a blue dot) and the target return (marked with a red dot), and would be identified by the traditional method of object identification.

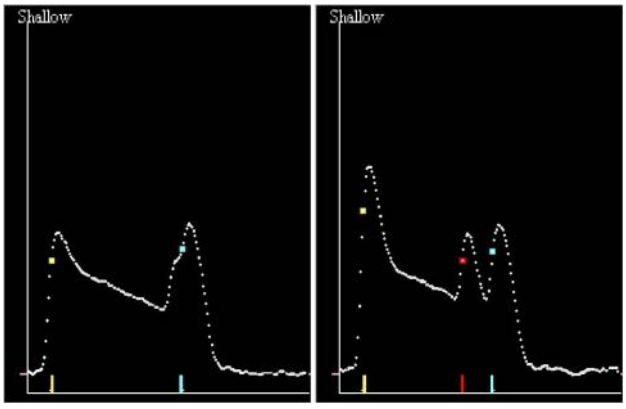

Figure 2: Sample waveforms from two targets of different size sitting side by side under about 9 m of water.

However, the waveform produced by the 1-m cube showed only a single peaked bottom return with an inflection at the leading edge of the bottom signal.

This kind of waveform would not be tagged by any of the traditional algorithms; therefore it would derive a normal bottom elevation (or water depth) without notice. As a matter of fact, the location of the blue dot indicates that this waveform will result in an elevation (or water depth) referenced to the true bottom, which means the existence of the target is totally ignored. No matter how carefully the bottom surface and lidar point clouds are examined and analyzed, this 1-m cube would be completely invisible.

The enhanced object detection algorithm takes into consideration the situation shown in Figure 2, as well as many other variants of distorted bottom return signals from bottom features. The basic approach of the enhanced object detection algorithm is that any illuminated objects will distort the waveforms, which will then trigger a sophisticated algorithm for object recognition.

3.2. Object categorization and case definitions

Case 1: These objects are features that are larger than the laser footprint. ***Figure 3*** illustrates the categorization of Case 1 objects, where the sizes are significantly larger than the laser footprint size (~ 2 m). The numerous features on the sea floor are easily identifiable in the lidar point clouds; although individual waveforms reflected from these features do not show any differences than those from flat sea bottom, such as the sample waveform inset in the image. The Case 1 features represent the conventional objects that many people refer to (Smith 2006), but they only account for a very small portion of the objects detectable by the SHOALS system. Identification of the Case 1 object is based on spatial analysis, and it is applicable for larger features as well as cases where return signals from the object surface area overshadow those of the water bottom in optically deep water. The Case 1 identification also depends on object definition and selection criteria.

Case 2: Any objects of comparable size to the laser footprint (i.e., similar to a 2-m cube) will mostly be identifiable by the traditional method of object detection. In Figure 4 we show detection of a Case 2 object.

The sample waveform clearly shows a separation between object return and bottom return, which is the criteria for Case 2 object detection. This object detection strategy works very well when the object size is comparable to the laser footprint size on the bottom. This ability to detect an object within the laser footprint is one of the major characteristics of the airborne bathymetric lidar (such as SHOALS) compared to the multibeam echo sounder (MBES), although the latter has much greater point density to detect Case 1 objects. Because SHOALS maintains a surface laser footprint of approximately 2 m that expands further in the water column, often significantly, the return signal from an object with size comparable to the laser footprint is usually followed by a signal reflected from the sea bottom. Such a physical phenomenon does not stop the feature from being detected by properly-designed pulse -detection software. Indeed, this very beam spreading actually increases the feature detection probability in shallow water for limited spot spacing. As part of the SHOALS object detection strategy, any waveforms with reliable second returns are categorized as object waveforms, which trigger the Case 2 object detection. ***Figure 4*** shows the detection of a 2-m cube under about 11 meters of water

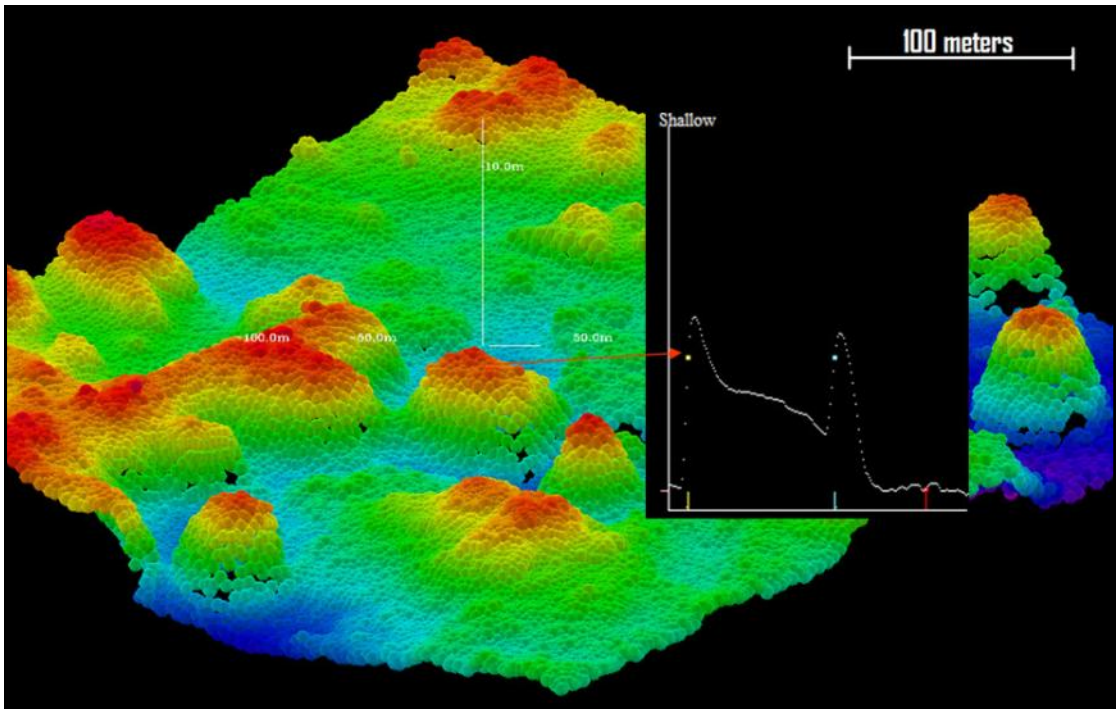

Figure 3: llustration of a Case 1 object in a lidar point cloud of a complex sea bottom topography, with a sample waveform from the object surface.

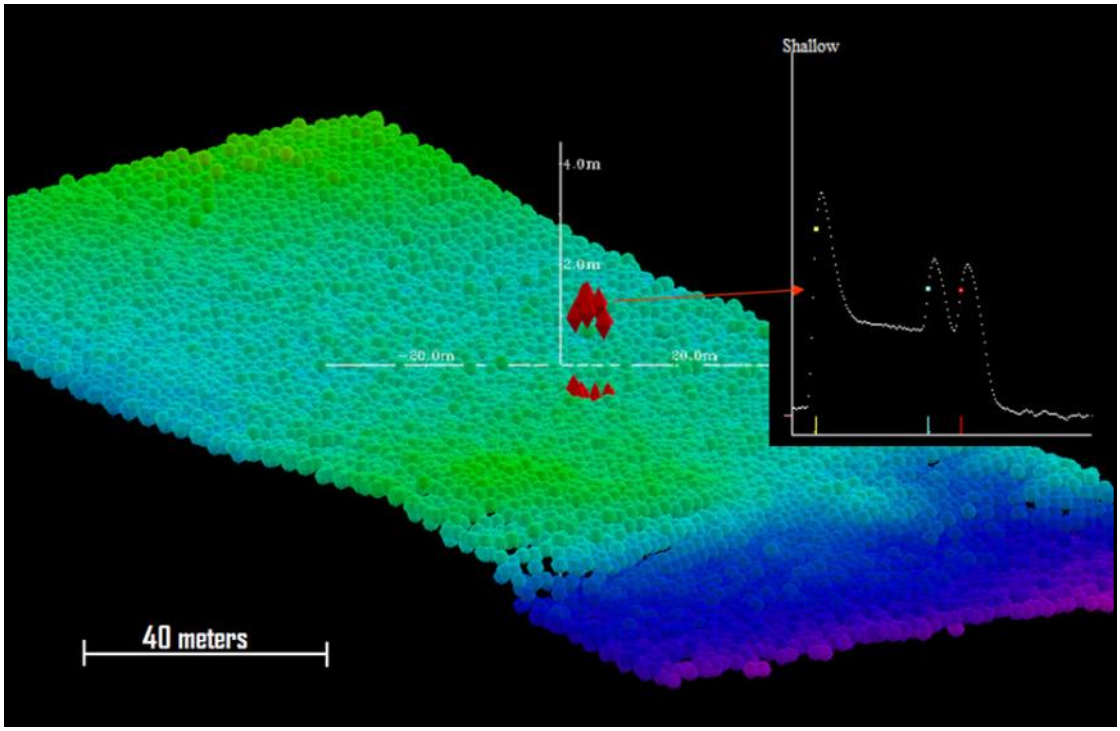

Figure 4: Detection of a 2-m cube under about 11 m of water

Case 3: All objects other than those captured by Case 1 and Case 2 will be designated as Case 3 objects, which include objects with dimensions ranging from 2-m cubes (not captured by Case 2) to objects as small as 0.5-m cubes. For Case 3 objects, there are many examples and variants, which are characterized by object signatures other than clear separation between the object return and bottom return. ***Figure 5*** shows a case where four lidar soundings were identified and automatically highlighted as small objects by the enhanced object detection algorithm, with waveforms (from two different flightlines) displayed under the point cloud. A sub-meter small object is detected and automatically highlighted by the yellow triangles.

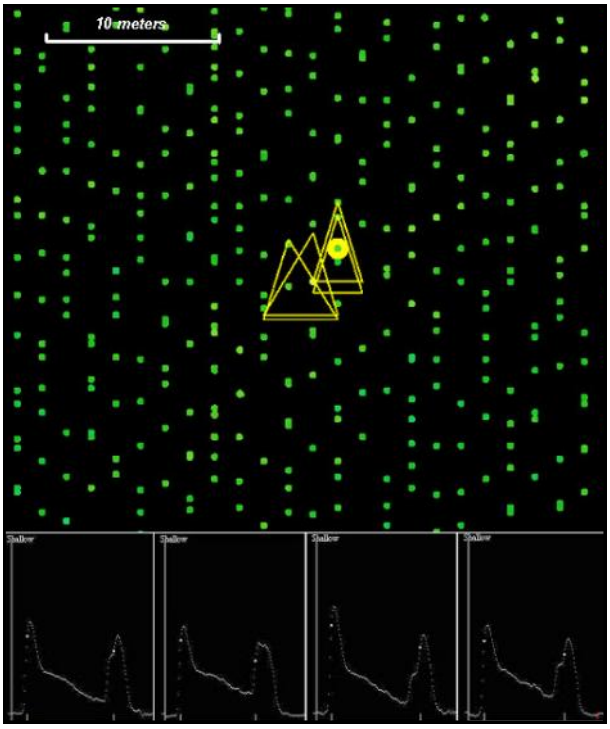

Figure 5: Lidar points from two overlapping flightlines (300 m altitude, 3 m × 3 m spot spacing).

In the past, this kind of feature was not detectable; therefore, the corresponding small object would be totally ignored. However, with the enhanced object detection algorithm, the subtle signatures of even sub-meter objects can be detected in the bottom return signals. If a survey is properly planned to ensure 100% bottom illumination, objects larger than a certain detection threshold will be captured. Such detection thresholds are currently set at 1 m and 0.5 m respectively for different detection sensitivities in the enhanced object detection algorithm.

Noteworthy also is that the recognition of Case 2 and Case 3 objects is based on a single waveform, which means that the SHOALS enhanced object detection algorithm observes small objects within the small field of view (FOV) of the receiver telescope. This is an innovative concept in contrast to the conventional wisdom of applying the "Nyquist criterion" (Guenther 2007) (Smith 2006). The SHOALS configuration of relatively large laser footprint and multiple FOV has effectively increased the object detection capability if the return signal from each individual lidar sounding is carefully analyzed. Based on the understanding that the transmitted laser pulses have constant shape and that the propagation-induced pulse stretching is reasonably small and predictable, the enhanced object detection algorithm is capable of detecting distortions to the bottom return induced by bottom features in the scale of 0.5 m (about 5 ns in the digitizer waveform scale). This allows the detection of small objects at similar scale.

Overall, the enhanced capability of SHOALS object detection is a result of both hardware advancement and algorithm development. The hardware advancement results in higher laser pulse repetition rates, higher point density and complete bottom illumination, whereas the algorithm enhancement ensures effective identification of bottom features from their subtle signatures.

4. Situation studies

There are numerous examples to demonstrate SHOALS' ability and efficiency in detecting bottom features and anomalies, including field trials using manmade targets as well as comparison analysis between lidar and MBES surveys.

In the 2003 acceptance tests of the SHOALS-1000 system in Florida (LaRocque *et al.* 2004), ten 2-m cubes and six 1-m cubes were constructed and placed on the sea bottom in two east-west lines named "southern target line" and "northern target line" at depths ranging from 5 m to 28 m, as illustrated in ***Figure 6***. Overall, there were four 2-m cubes placed in the "northern target line", and six 2-m cubes and six 1-m cubes placed in the "southern target line". Multiple flightlines were flown over these two target lines with various survey patterns.

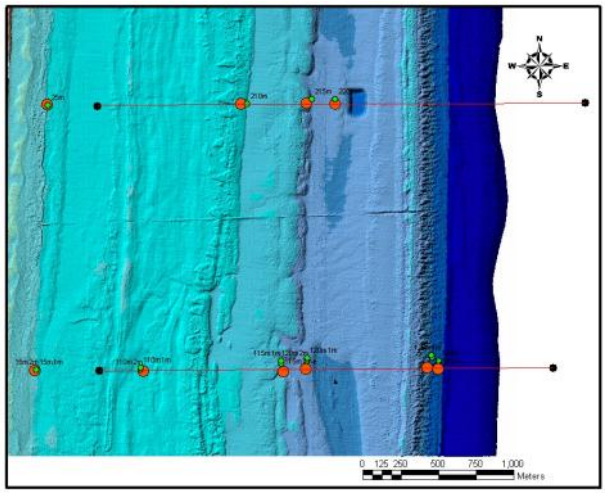

Figure 6: Placements of the bottom targets.The red dots mark the planned locations for target placements, and the green dots are the actual locations of the target.

During the one month period of the 2003 acceptance tests, multiple flights in different days were conducted along the two target lines in order to study the SHOALS object detection capability.

Other than the variable water depths of target placements (i.e., from 5 m to 28 m) and target sizes (i.e., 1-m cube and 2-m cube), different survey patterns were chosen for various flight missions, with point densities of 2 m × 2 m, 3 m × 3 m and 4 m × 4 m. Such arrangements had the intention of examining the system's target detection capability under variable conditions.

The data collected in the 2003 field trial were lately processed for object detection analysis, using our enhanced object detection algorithm, combined with the technique of second depth recognition. Our results indicated that almost all of the underwater targets were successfully identified by our automated algorithm. As an example, ***Figure 7*** shows the 3D lidar point cloud of a dataset collected over the "northern target line", with three targets clearly detected and highlighted (in red color and circled), which are 2-m cubes placed in water depths from about 12 meters to 21 meters. A camera picture is inset to illustrate the size of the 2-m target, and a sample waveform is also displayed to exemplify a typical signature in the target waveform.

Overall, more than 80 flightlines were flown over the targets in various days throughout the field trial period. After processing all flightlines using our latest object detection algorithm, we can summarize the probabilities of detecting the 2-m cubes and 1-m cubes, under different lidar point densities and varying water depths. The detection probability of a target was calculated based on the ratio between the number of flightlines detecting the target (using the criterion that at least one or more target waveform was automatically identified and highlighted by our automated object detection algorithm) and the number of flightlines flown over the target area when the target is in place. According to the SFTF (South Florida Testing Facility), a few of the shallow targets collapsed or shifted positions during the trial period, especially due to tropical storm Erika which occurred in the middle of the trial period. Our analysis took into consideration that some targets might be absent during the specific surveys (with specific survey patterns). Therefore, the detection probabilities were labeled as "N/A" under the scenario when a mission with multiple flightlines collected over a presumed target location showed no sign at all of any target signatures. We are very confident that the cubes were simply not present for the N/A cases.

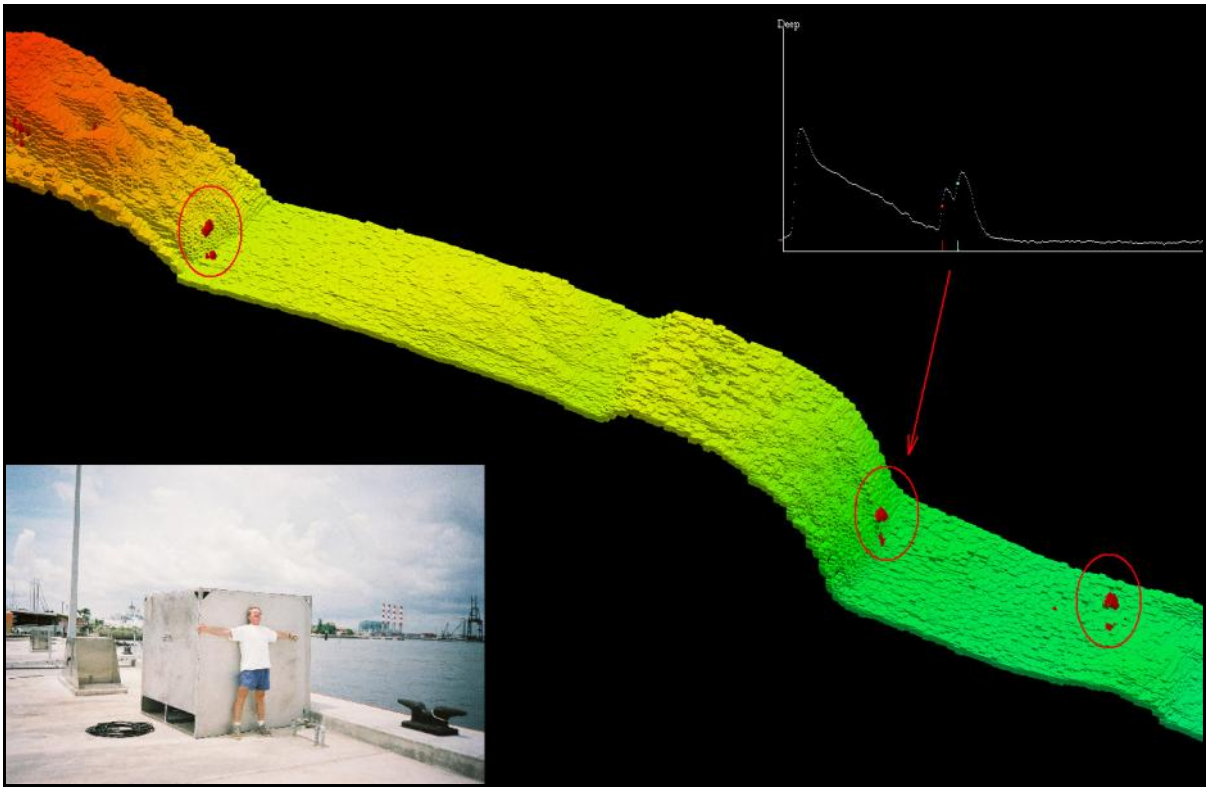

Figure 7: 3D view of lidar points from the "northern target line". Three 2-m targets are automatically identified and highlighted.

Table 2 summarizes our analysis on the detection probabilities for the 2-m cubes, which are those outlined in Figure 6. The six 2-m cubes in the southern target line are labeled from "1S" to "6S", with "S" denoting the "southern target line" and the incremental numbers indicating their sequence from the closest to the farthest off shore. With the same naming convention, the four 2 -m cubes in the northern target line are labeled from "1N" to "4N". The second column shows the water depths where individual targets were located, and the third, fourth and fifth columns display the detection probabilities of all targets under different survey patterns. The numbers in brackets are the number of automatic detections divided by the number of flightlines over the target (each flightline or pass is allowed a maximum of one detection). The 2-m cubes were analyzed with a 1-m detection sensitivity; the 1-m cube data were analyzed with a 0.5-m sensitivity.

Note that water clarity did play a role in the detection of the cubes. The SHOALS systems have been demonstrated to measure water depths more than three times the Secchi Depth (LaRocque, *et al*. 2004). For the test cases above, we used the criteria of the cube Bottom Depth being no deeper than approximately 2/3 of the lidar bottom extinction depth for that day. Essentially, we are saying that with a lidar performance of three times the Secchi Depth, the cubes will be found reliably within two Secchi depths. It is evident from Table 2 that SHOALS has almost 100% probability to detect automatically the 2-m cubes under the specified conditions, with water depths ranging from 5.5 m to 28.3 m and lidar point density from 2 m × 2 m to 4 m × 4 m. Although there is indication that the detection probability decreases once spot spacing exceeds 3 m × 3 m, it is almost certain that SHOALS is capable of meeting the IHO-1 requirement for object detection if the water clarity is such that the cube depth is within 2/3 of the extinction depth.

Table 2: Target detection percentages for 2-m cubes

Target ID	Bottom Depth	2 × 2 Spot Spacing	3 × 3 Spot Spacing	4 × 4 Spot Spacing
1S	5.6 m	100% (7/7) [A]	N/A (0/15) [B]	N/A (0/17) [B]
2S	10.1 m	100% (9/9) [A]	100% (10/10) [C]	100% (9/9) [C]
3S	19.3 m	100% (17/17)	100% (6/6) [D]	100% (8/8)
4S	22.7 m	100% (18/18)	100% (6/6) [D]	91% (10/11)
5S	25.6 m	100% (10/10)	100% (6/6) [D]	100% (13/13)
6S	28.3 m	100% (11/11)	100% (6/6) [D]	73% (8/11)
1N	5.5 m	N/A (0/4) [E]	100% (7/7) [F]	100% (8/8) [F]
2N	12.4 m	100% (3/3)	100% (6/6) [F]	100% (8/8) [F]
3N	19.5 m	100% (5/5)	100% (16/16)	100% (17/17)
4N	20.5 m	100% (3/3)	100% (11/11)	93% (13/14)

Table 2 Notes:

[A] The 2 × 2 pattern has a narrower swath than the 3 × 3 and 4 × 4 patterns. Some of the 2 × 2 swaths missed the cube locations, leading to a smaller sample set.

[B] This 1S target collapsed, was repaired and reinstalled on Aug 11. The 2 × 2 flights were flown on the 12th. The 3 × 3 and 4 × 4 flights were flown before Aug 11 when the target was not present or after Tropical Storm Erika of Aug 14. It is suspected the cube was moved out of the search area by the storm.

[C] The location of the 2S target was moved NW by 70 meters by TS Erika. The 3 × 3 and 4 × 4 flights were after the storm and found the cube in this different location from the 2 × 2 flights.

[D] The smaller sample numbers for these cubes in the 20 to 30-m depth range is due to the decreased water clarity after Aug 14.

[E] This 1N target also collapsed. The 2 × 2 flights occurred when the target was not present.

[F] These targets were not observed again after flights on Aug 5. The later flights were after the storm and if the target was reinstalled, it must have moved as it was not detected at all.

Table 3 summarizes our analysis on the detection probabilities for those 1-m cubes placed in close proximity to the 2-m cubes along the "southern target line", as outlined in ***Figure 6.*** All six 1-m cubes identified in our analysis are associated with 2-m targets from 1S to 6S, therefore these 1-m cubes are labeled accordingly. The second column of the table shows the water depths associated with individual targets, and the third, fourth and fifth columns display the detection probabilities of these targets under different survey patterns.

Table 3 reveals that SHOALS is capable of automatically detecting 1-m cubes under most cases when the survey pattern has a lidar point density of 2 m × 2 m. Although the detection statistics for the 1-m cubes are not as good as for the 2-m cubes, it is still a remarkable performance by the SHOALS system to find most of the 1-m cubes located on the sea floor with water depth ranging from 5.9 m to 27.6 m, owing to the enhanced object detection algorithm. The statistical analysis indicates that SHOALS is capable of meeting the IHO special order with 2 m × 2 m point density in water depth of more than 20 meters (if the water is sufficiently clear).

The statistical results of target detection for the 2003 field trial support and surpass what was predicted in the analytical studies (Guenther *et al* 1996). Particularly, owing to the enhanced object detection algorithm, the capability of detecting 1-m cubes or those objects with lower vertical height is drastically enhanced, which allows SHOALS to meet IHO Special Order in clean water condition.

Another important study to demonstrate SHOALS object detection capability is from a comparison analysis between MBES and SHOALS in surveying an area full of bottom rocks and pinnacles at Saipan in the Northern Mariana Islands. ***Figure 8*** illustrates the two overlapped areas surveyed by SHOALS in 2006 and by MBES in 2007 (Elenbaas 2008), both of which covered a dredged navigation channel west of Saipan. One of the major characteristics of these surveyed areas is their complex bottom topographies at the west entrance of the channel, such as shown in ***Figure 9***. The water clarity at the site was favorable for bathymetric lidar surveys, and the SHOALS mission was performed with 3 m × 3 m spot spacing, therefore the results of the SHOALS survey represent a classical performance of the system and should meet IHO-1 standards for both position accuracy and object detection.

In 2008, an analysis was presented entitled, "A Comparison of Object Detection Using Airborne Lidar and Acoustic Sensors" which addressed the Saipan surveys at the 9th Annual JALBTCX Coastal Mapping & Charting Technical Workshop in San Francisco, CA, and summarized findings by using a spatial analysis tool for object selection developed by NAVOCEANO (Elenbaas 2008). In this study, an overlapping area of about 1.64 km^2 between SHOALS and MBES was chosen, and then the object list selected from SHOALS surveys was compared with the object list determined by NOAA's acoustic survey team. The findings indicated that SHOALS found 535 objects in the area, whereas NOAA's team only selected 162 objects.

Table 3: Target detection percentages for 1-m cubes

Target ID	Bottom Depth	2 × 2 Spot Spacing	3 × 3 Spot Spacing	4 × 4 Spot Spacing
1S(1m)	5.9 m	100% (11/11)	63% (5/8)	67% (2/3)
2S(1m)	10.2 m	100% (10/10)	70% (7/10)	63% (10/16)
3S(1m)	19.5 m	81% (13/16)	0% (0/6)[G]	0% (0/11)[H]
4S(1m)	22.8 m	100% (18/18)	100% (6/6)	45% (5/11)
5S(1m)	25.4 m	67% (6/9)	33% (2/6)	17% (1/6)
6S (1m)	27.6 m	43% (3/7)	40% (2/5)	38% (3/8)

Table 3 Notes:

[G] The 3S 1-meter cube was automatically selected well with 2 × 2 spacing. For the 3 × 3 spacing it was visually observed at least three times in the waveforms but it was not selected by the algorithm because the cube/bottom was at the limit of the recording of the Shallow Channel. Note also that in the same flightline, the return signal from this 3S 1-m cube was noticeably and consistently less than the return signal of the deeper 4S 1-m cube. This indicates either a lower reflectivity of the 3S 1-m cube or perhaps a partial submersion of the 3S cube.

[H] The 4 × 4 spacing data also showed the cube visually at least twice but it was not automatically detected. The water clarity after the storm of Aug 14 definitely affected the ability to find the 1-m cubes.

Among the SHOALS selected objects, 133 of them coincided with NOAA's object list, with 29 unmatched. However, after carefully studying the 29 unselected objects, they saw that SHOALS actually detected 28 of them, but they were not selected due to the criteria used. It is noteworthy that the spatial analysis tool for object selection used by NAVOCEANO made use of the SHOALS' post-processing results of the second depth detection to aid the spatial object selection, but our latest enhancements to the object detection algorithm further improved the sensitivity.

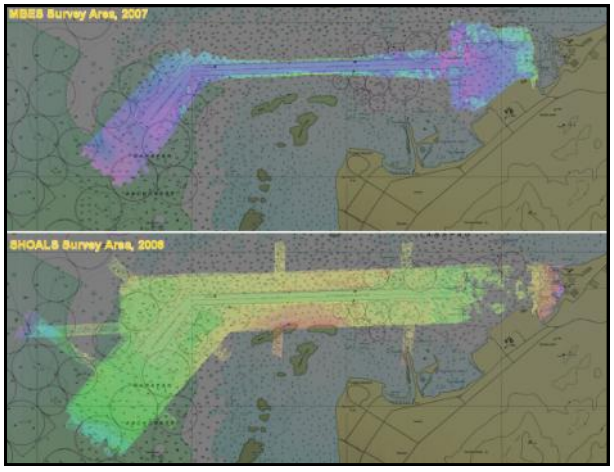

Figure 8: Coverage areas of SHOALS survey in 2006 and MBES survey in 2007 at Saipan.

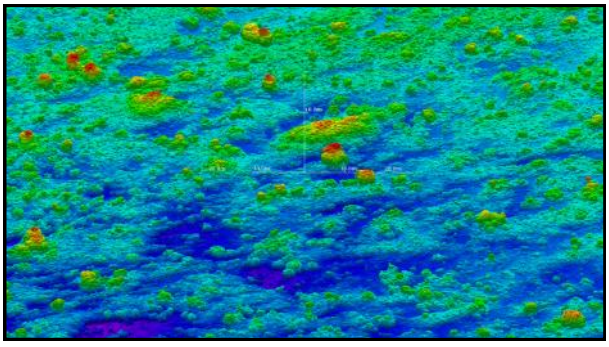

Figure 9: 3D point cloud of MBES data at the entrance area of the Saipan navigation channel..

The same SHOALS data was also processed with our latest object detection algorithm, together with our own object selection tool developed under the envelope of the SHOALS GCS package. ***Figure 10*** illustrates a 2D point cloud at the west entrance area of the dredged channel, color-coded by water depth. The red dots mark locations of the GCS-selected objects that were detected multiple times by waveforms with object signatures (highlighted with yellow triangles around the lidar points) and the blue dots locate those GCS-selected objects that were detected by a single object waveform.

In the case of the red dots, a spatial clustering algorithm was used to group the multiple detected lidar points by their close proximity, and to mark the centric position of the group.

The enhanced object detection algorithm further improved the SHOALS capability in detecting smaller objects on the seafloor, which resulted in many more objects being detected in the Saipan data by SHOALS. Analysis indicated that the new object list automatically selected by our enhanced object detection algorithm encompassed all objects spatially detected by NAVOCEANO and also marked 15 of the 29 missing objects from the NOAA object list. The locations of the remaining 14 "missing objects" in the NOAA list were also examined. For some presumed MBES objects, the selection was a bit dubious, and for the rest of the fourteen, it is clear they could have missed manual selection had different criteria been used.

Comparing object lists can be quite subjective, especially in the case of Saipan, because it depends on the definition of objects, including object sizes, dimensions and least depths, etc. For our spatial clustering algorithm, the definition of object separation also played a role in the final object list, namely, if two objects are sitting together, they could be counted as one bigger object. Also, our enhanced object detection algorithm has user input about the detection sensitivity for objects of different sizes. Table 4 and Table 5 summarize our findings by using different algorithm settings to process one data set from Saipan. It resulted in a variable amount of objects detected due to the bottom complexity with numerous objects in very close proximity.

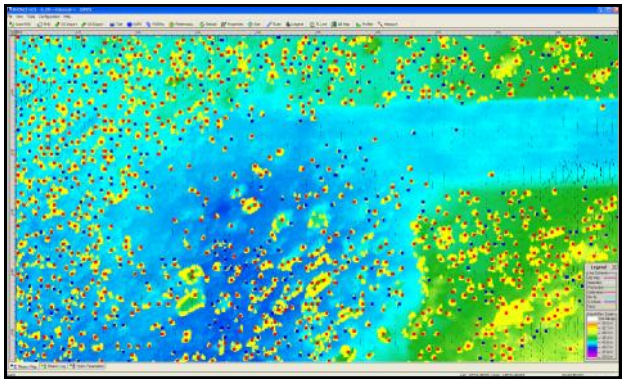

Figure 10: 2D point cloud of SHOALS data in the Saipan navigation channel, with red dots identifying objects detected by multiple hits, and blue dots identifying objects by a single hit.

Table 4 shows the object selection statistics with different detecting sensitivities, which were set at 2 m, 1 m and 0.5 m in vertical heights. Obviously, the number of detected objects increases when decreasing the threshold of vertical height for object identification. Also in the table are the statistics about objects with multiple lidar hits and a single hit. The criterion for object separation in this analysis is about 7.5 meters (namely, using a cell size of 5 meters in the spatial analysis).

Table 4: Object Selection statistics with different object detection algorithm sensitivities

Detection Category	Sensitivity I (~ 2 m)	Sensitivity II (~ 1 m)	Sensitivity III (~ 0.5 m)
Multi-hits	1527	4098	6265
Single-hit	1440	2159	1908
Total	2967	6257	8173

Table 5 shows the object selection statistics with different cell sizes in spatial analysis. The number of detected objects decreases when increasing the object separation requirement, because some of the smaller objects in close proximity could be grouped into a larger object. Also in the table are the statistics about objects with multiple lidar hits and a single hit. The object detecting sensitivity was set at 1 m.

Table 5: Object selection statistics with different cell sizes

Detection Category	3 m cell size (4.5 m spacing)	5 m cell size (7.5 m spacing)	7 m cell size (10.5 m spacing)	9 m cell size (13.5 m spacing)
Multi-hits	4379	4098	3487	2856
Single-hits	4360	2159	1143	626
Total	8739	6257	4630	3482

The study with Saipan data demonstrated SHOALS' ability in rapid reconnaissance of small underwater obstructions of variable sizes in natural situations, with great efficiency. Although there is no doubt that the latest high-resolution multi-beam sonars have much greater point density than lidar, thus superior object detection performance, SHOALS is very effective in detecting underwater objects if a sophisticated algorithm is applied. It is understandable that both sonar and lidar have their areas of optimum utility based on survey requirements, safety, cost, and speed-of-coverage considerations. Under clean water conditions, SHOALS has supremacy of much greater coverage rate than sonar and can easily meet IHO-1 requirements in position accuracy and object detection.

There are other situation studies to further demonstrate SHOALS' object detection capability under varying water conditions, including not so clean water. One of those studies was from Shilshole Bay, Seattle, WA, where the extinguishing depth was less than 12 meters during two of the SHOALS surveys conducted in 2005 and 2007. In these two surveys, there were two sets of pre-installed targets (in 2005) with dimensions of 2 m × 2 m × 2 m, 2 m × 2 m × 1 m and 1 m × 1 m × 1 m under water depths of about 7 meters and 12.5 meters respectively (Lockhart *et al* 2005). By using the enhanced object detection algorithm, two of the larger targets (i.e., 2 × 2 × 2 and 2 × 2 × 1) under 7 meters of water were automatically detected and highlighted, together with many other natural objects identifiable by examining the multibeam coverage (Lockhart *et al* 2005). The results from Shilshole Bay, as well as many other local flights over Lake Ontario, clearly indicate that SHOALS is capable of meeting IHO-1 requirements (within its extinguishing depth) even if the water clarity is not optimal for bathymetric lidar surveys.

5. Discussion

Small object detection is a very important part of hydrographic surveys, but it is also complicated for both sonar and lidar because the detection probability depends on multiple factors. With the addition of the enhanced object detection algorithm, SHOALS has significantly improved its capability of detecting smaller objects. However, its dependency on water clarity still remains. Empirically, using the shallow depth channel, SHOALS is capable of detecting objects greater than 1-m cubes within 2-Secchi depths 100% of the time. Such empirical results can be explained by the fact that the shallow green channel of the SHOALS system has a limited FOV of 15 mrad, which enhances object contrast in its measurable depth range of about 0-17 m. The limit of 2-Secchi depths relies on the achievable sensitivity of the enhanced object detection algorithm that allows reliable differentiation of the object return from the bottom return. As seen in Tables 2 and 3, the 1-m and especially the 2-m cubes are also well detected in the deep green channel which has a much larger FOV. Since this particular data set was acquired, the detectability in the deep channel has been further enhanced by the use of a faster detector (LaRocque, Yang 2010).

The analytical study (Guenther *et al.* 1996) assumed infinite FOV of the receiver channel, although the paper mentioned that limited FOV would increase the object contrast. As a matter of fact, the FOV plays a very significant role in object detection. For example, an altitude of 300 m results in an observing window of only 4.5 m in diameter with a 15 mrad FOV. This implies that the effective footprint size visible to the receiver is reduced to a much smaller size than that of the expanded laser footprint (Guenther 1985) (Kopilevich *et al.* 2005). Such an impact of the FOV further consolidates SHOALS' ability to detect objects greater than 1-m cubes under most environmental conditions, with unit probability to about 2-Secchi depths.

Another point of discussion is laser beam expansion in various water conditions, which has sometimes simply been assumed to be approximately half of the water depth. This assumption is believed to be an overestimate in clear water. Studies (Guenther 1985) (Kopilevich *et al.* 2005) indicate that expansion of the laser beam could be as low as 20% of the water depth in optically clear water, which significantly decreases the effective laser footprint on the water bottom. If that is the case, it also explains the enhanced contrast of object return signal versus the return signal from the surrounding bottom.

Based on the above analysis, combined with the requirement for 100% bottom illumination, the practical guidelines for rapid reconnaissance of small underwater obstructions would be:
1) a 300-m altitude, 3 m × 3 m spot spacing pattern is efficient and optimized for detecting objects larger than 1-m cubes;
2) a 300-m altitude, 2 m × 2 m spot spacing pattern provides a thorough inspection of all underwater small objects, and has the capability of detecting objects as small as 0.5-m cubes in very clean water;
3) object detectability depends on water clarity, but the rule of thumb is that any objects within 2-Secchi depths will be reliably detected with unit probability.

The enhanced object detection algorithm is based on a signal observed within a small FOV, which assumes a flat water bottom. There are cases where distortions of bottom returns are triggered by sudden bottom slopes, which can lead to mislabeling such bottom anomalies as small objects. Usually, mislabeled bottom anomalies are associated with very rugged water bottoms or neighboring areas surrounding a much larger bottom feature, where user inputs through 3D editing are required to identify isolated objects. Nevertheless, the enhanced object detection algorithm is capable of highlighting all suspected lidar points.

During development of the enhanced object detection algorithm, major improvements were made to the traditional method of object identification. Initially, any lidar return with a second depth was classified as an object, which resulted in a very high rate of "false alarms" due to noisy waveforms, especially within the water column. Such false alarms, sometimes dominating the highlighted suspects, overshadowed the ability to observe true bottom features, and degraded the overall performance of the system's object detection capability. With the new enhanced object detection algorithm, any water column-induced second depth is carefully analyzed automatically to reject false alarms.

Overall, SHOALS' object detection capability is built on successfully identifying three different types of bottom features: Case-1 objects, which are obvious in the lidar point cloud; Case-2 objects, which are identified by distinguishable object and bottom returns using the traditional pulse location algorithms; Case-3 objects, which differentiate bottom anomalies by examining distortion in the bottom returns. Case-3 handles all situations that are not handled by both Case-1 and Case-2, and enables detection of objects as small as 0.5-m cubes.

6. Conclusion

Both empirical and analytical results indicate that SHOALS is highly capable of detecting small objects underwater. Empirical studies indicate that, under clear water conditions, SHOALS exceeds IHO-1 requirements for underwater object detection and, with proper survey planning, can also meet IHO Special Order requirements.

Considering the efficiency and cost effectiveness of using airborne bathymetric lidars such as SHOALS, it is obvious that this is the technology of choice for the rapid reconnaissance of small underwater obstructions in shallow coastal water.

The enhanced object detection capability also suggests that the SHOALS system has great potential for military applications in the rapid reconnaissance of underwater mines and any other objects of interest as small as 0.5 m in diameter.

7. Acknowledgements

The authors wish to thank the Joint Airborne Lidar Bathymetry Technical Center of Expertise (JALBTCX) for the use of data and imagery from the 2003 CHARTS field trials. In addition, Bill Elenbaas and his colleagues of NAVOCEANO shared their data, imagery and analysis on the Saipan data. The authors also wish to thank Michael Broadbent and Fugro Pelagos for their survey data and target information over Shilshole Bay, Seattle, WA. Special thanks go to Wenbo Pan of Optech for her tremendous efforts in processing and analyzing all the data from the SHOALS 2003 field trial to produce the recent statistical results in that case study.

References

Elenbaas, B. (2008) A Comparison of Object Detection Using Airborne Lidar and Acoustic Sensors, *9th Annual JALBTCX Coastal Mapping & Charting Technical Workshop, San Francisco, CA*, 17-18.

Guenther, G.C. (2007). *A letter to the editor, International Hydrographic Review*.

Guenther, G.C., Eisler, T.J. Riley, J.L. and Perez, S.W. (1996). *Obstruction detection and data decimation for airborne laser hydrography, Proceedings, 1996 Canadian Hydrographic Conference, Halifax, N.S.* 51-63.

Guenther, G.C., (1985). *Airborne laser hydrography: system design and performance factors, NOAA professional paper series, 1. Rockville, Md: U.S. Dept. of Commerce, National Oceanic and Atmospheric Administration, National Ocean Service, Charting and Geodetic Services*, 385.

IHO *(International Hydrographic Organization) IHO Standards for Hydrographic Surveys, Special Publication No. 44, 5th Edition, Feb 2008.*

Kopilevich, Y., Tuell, G., Feygels V. (2005*). Aspects of resolution and target detection, 6th Annual Airborne Coastal Mapping and Charting Workshop, July 2005, Philadelphia, PA.*

LaRocque, P.E., Yang, E. (2010). *Enhancements to the New SHOALS-3000 System, International Lidar Mapping Forum, March 2010, Denver, Colorado.*

LaRocque P.E., Banic, J.R. and Cunningham, A.G. (2005). *CHARTS Upgrade (SHOALS-3000T20E) Design Description and Field Testing, 6th Annual JALBTCX Coastal Mapping & Charting Technical Workshop*, Philadelphia, PA, July 12-13, 2005.

LaRocque P.E., Banic, J.R. and Cunningham, A.G. (2004). *Design description and field testing of the SHOALS-1000T airborne bathymeter, Proc. SPIE Vol. 5412, Laser Radar Technology and Applications IX; Gary W. Kamerman; Ed. p162-184.*

Lockhart, C., Arumugam, D., Millar, D. (2005). *Meeting Hydrographic Charting Specifications with the SHOALS-1000T Airborne LiDAR Bathymeter, Proceedings of the 2005 U.S. Hydrographic Conference, San Diego, CA.*

Smith, S.M. (2006). *Empirical Object Detection Performance of LIDAR and Multibeam Sonar Systems in Long Island Sound, International Hydrographic Review Vol. 7 No. 2, July 2006.*

West, G.R. and Lillycrop, W.J. (1999). *Feature Detection and Classification with Airborne Lidar - Practical Experience, Proc. Shallow Survey 99,* October 18-20, Sydney, Australia.

Yang, E., LaRocque P.E., Guenther G.C., Reid D., Pan W., Francis K. (2007). *Shallow water depth extraction – progress and challenges, Proceedings of the 2007 U.S. Hydrographic Conference,* Norfolk, VA.

Biographies of the Authors

Eric Yang is a scientist with great enthusiasm in the study of various lidar applications. Based on his knowledge of the lidar sensors and lidar physics, Eric has been actively involved in advancing the bathymetric lidar technology and its applications. In 2009, Eric was awarded the inaugural "Technical Achievement Award" by the Joint Airborne Lidar Bathymetry Technical Center of Expertise (JALBTCX). Eric received his BSc in physics from Peking University and his MSc in geological sciences from McMaster University. He also spent three years of Ph.D. study at McMaster University in applied physics.

Dr. Paul LaRocque is currently the Director of Advanced Technology at Optech, the wing of the company that specializes in research and development. In the past he has been the Technical Manager for a variety of Optech systems: atmospheric lidars, terrain mappers, and most notably for the SHOALS family of airborne lidar bathymeters. This began in the early 90's with the SHOALS 200 system, which has evolved lately into the new SHOALS 3000 system. Paul received his doctorate in Laser Spectroscopy from the University of Toronto in 1985.